Iranian Journal of Geophysics, Vol. 9, No. 5, 2016, Page 57-71

Application of surface-derived attributes in determining boundaries of potential-field sources

Mohammad Barazesh[1], Seyed-Hani Motavalli-Anbaran[2]*, and Hojjat Ghorbanian[1]

[1]*M.Sc. Student, Institute of Geophysics, University of Tehran, Iran*
[2]*Assistant Professor, Institute of Geophysics, University of Tehran, Iran*

(Received: 12 August 2015, accepted: 20 October 2015)

Abstract

This paper describes an edge detection method based on surface-derived attributes. The surface-derived attributes are widely used in the interpretation of seismic data in two main categories: (1) derivative attributes including the dip angle and the azimuth; (2) derivative attributes including curvature attributes.

In general, the magnitude of the normal curvature of a surface (curvature attributes) can be expressed in terms of derivatives of that surface which are called the first and second fundamental forms of the surface. For a quadratic surface which fits data, it is shown that the dip-angle equation in the interpretation of the seismic data is similar to the horizontal gradient magnitude (HGM) equation in the interpretation of potential field data. Among the infinite number of curvature attributes, a few of them which are suitable for edge detection are shown. The coefficients of a quadratic surface are calculated using the least square method. At a particular point, the attributes are obtained using these coefficients. Zero contours of most positive curvature and the determinant of the curvature matrix delineate the location of the edges of anomalies. The shape index attribute quantitatively reflects the local shape of the surface over sources in terms of cap, dome, ridge, saddle, rut, trough and cup. Here, the maximum curvature is introduced as a new technique to detect the horizontal location of anomalies.

First, the introduced attributes were applied to the noise-free synthetic data. Then, the data with the noise added were used to check the stability of the method. In the presence of high-level noise, this method was successful in determining boundaries of the anomalies. Zero contours of the most positive curvature, the determinant of curvature matrix and the maximum curvature properly illustrate the linear features within the mapped surface. The results of using surface-derived attributes were compared with tilt angle and HGM filters. This comparison showed that zero contours of the most positive and maximum curvature attributes are approximately matched with zero contours of the tilt angle and maximum values of HGM. Finally, this method was used for real data from Mobrun massive sulfide ore of Canada. MATLAB software was used for programming and calculating the required parameters of this method.

Keywords: Surface-derived attributes, potential field data, most positive curvature, maximum curvature, shape index, zero contours.

*Corresponding author: Motavalli@ut.ac.ir

1 Introduction

One of the most important issues in the interpretation of potential-field data is to determine the horizontal location of the sources. Many methods have been designed for this purpose using simplified assumptions on the source to locate the complicated sources. Zero contours of the tilt angle (Miller and Singh, 1994) coincides with the edges of sources. Using vertical derivatives (Cooper and Cowan, 2003) also enhances the edge of the anomalies. The total-horizontal derivative of the tilt angle (THDT) (Verduzco et al., 2004), horizontal gradient magnitude (HGM) (Grauch and Crodell, 1987), analytical signal (Nabighian, 1972) and the theta map (Wijins et al., 2005) have maximum values on the boundary of anomalies. Despite a widespread use, all of these methods have some limitations. For example, when the magnitude of the analytic signal, HGM, tilt angle, or THDT is applied to the anomalies, the continuity of small geological features becomes inadequate for interpretation because of the variation in magnitude of the anomalies due to varying source to observation distances (Santos et al., 2012).

Roberts (2001) has presented a number of surface-derived attributes and their formula in seismic applications. The dip angle (from the first derivative attributes) and curvature attributes (from the second derivative attributes) of the surface-derived attributes are able to display properly the linear features of the mapped surfaces. Oruç et al. (2013) utilized eigenvalues of the curvature gravity gradient tensor (CGGT) to detect and outline edges of anomaly sources. These eigenvalues are the most positive and the most negative curvature attributes which introduced by Roberts (2001). Hansen and deRidder (2006) proposed the linear feature analysis based on the curvature of the total horizontal gradient of the total magnetic field.

In this study, the efficiency of the surface-derived attributes was evaluated to delineate the edges and boundaries of potential anomalies (Cevallos et al., 2013). Furthermore, the dip angle and the maximum curvature attributes were introduced as two new methods for detecting edges of anomalies.

2 Methodology

For gridded data, there are various methods for calculation of the attributes (especially curvature attributes). Roberts (2001) used the least square quadratic approximation to the mapped surface. In order to calculate the attributes at a particular point, a quadratic surface is fitted within 3×3 windows in a least square sense. The coefficients of quadratic surface (Eq. 1) within 3×3 windows centered on the grid point (i, j) are defined by the following equations (Philips et al., 2007):

$$Z = ax^2 + by^2 + cxy + dx + ey + f, \tag{1}$$

$$a = \frac{1}{2}\frac{\partial^2 Z}{\partial x^2} = \frac{1}{6(\Delta x)^2}[Z_{i+1,j+1} + Z_{i+1,j} + Z_{i+1,j-1} + Z_{i-1,j+1} + Z_{i-1,j} + Z_{i-1,j-1} - 2(Z_{i,j+1} + Z_{i,j} + Z_{i,j-1})], \tag{2}$$

$$b = \frac{1}{2}\frac{\partial^2 Z}{\partial y^2} = \frac{1}{6(\Delta y)^2}[Z_{i+1,j+1} + Z_{i,j+1} + Z_{i-1,j+1} + Z_{i+1,j-1} + Z_{i,j-1} + Z_{i-1,j-1} - 2(Z_{i+1,j} + Z_{i,j} + Z_{i-1,j})], \tag{3}$$

$$c = \frac{\partial^2 Z}{\partial x \partial y} = \frac{1}{4\Delta x \Delta y}[Z_{i+1,j+1} + Z_{i-1,j-1} - Z_{i+1,j-1} - Z_{i-1,j+1}], \tag{4}$$

$$d = \frac{\partial Z}{\partial x} = \frac{1}{6\Delta x}[Z_{i+1,j+1} + Z_{i+1,j} + Z_{i+1,j-1} - (Z_{i-1,j+1} + Z_{i-1,j} + Z_{i-1,j-1})], \quad (5)$$

$$e = \frac{\partial Z}{\partial y} = \frac{1}{6\Delta y}[Z_{i+1,j+1} + Z_{i,j+1} + Z_{i-1,j+1} - (Z_{i+1,j-1} + Z_{i,j-1} + Z_{i-1,j-1})], \quad (6)$$

where Z can be a gravity field or the intensity of the magnetic field; Δx and Δy are the grid interval in the x and y directions, respectively (Philips et al., 2007).

2.1 Surface-Derived Attributes

Surface-derived attributes are calculated directly from the surface. The most frequently used attributes in the interpretation of seismic data are the first derivative types (such as dip angle) (Marfurt, 2007). Curvature attributes are placed in another group which is called the second derivative attributes. The illustration of these attributes is very efficient in lineament and other subtle map features diagnosis, because these attributes delineate areas with high curvatures that closely agree with the edges of the anomalies.

2.1.1 Dip Angle

The dip angle can be derived using coefficients d and e, which are computed from Eqns. (5) and (6). This attribute extracts some of the main lineament included within the mapped surface:

$$\text{Dip Angle} = \tan^{-1}(\sqrt{d^2 + e^2}), \quad (7)$$

The values are limited between $-\pi/2$ and $\pi/2$. Therefore the maximum value is on the maximum dip over the edges of anomaly. This relationship is similar to the horizontal gradient magnitude (HGM) in terms of derivatives of the first order, except its values, because the inverse tangent function is limited and has dip saturation problem.

2.1.2 Curvature Attributes

Near massive bodies, it is clear that the potential field is severely bent. When these bodies become elongated in any direction, we expect that the curvature perpendicular to elongated direction has a maximum value (Roberts, 2001). Curvature quantitatively determines deflection from a straight line at a particular point on the curve. In mathematics, the magnitude of the normal curvature of surface ($Z(x,y)$) can be expressed in terms of derivatives as follows (Bergbauer, 2002):

$$K_n = \frac{\beta_{xx} + \beta_{xy}(dy/dx) + \beta_{yy}(dy/dx)^2}{\alpha_{xx} + 2\alpha_{xy}(dy/dx) + \alpha_{yy}(dy/dx)^2}, \quad (8)$$

where,

$$\begin{cases} \alpha_{xx} = 1 + (\frac{\partial Z}{\partial x})^2 \\ \alpha_{xy} = (\frac{\partial Z}{\partial x})(\frac{\partial Z}{\partial y}). \\ \alpha_{xx} = 1 + (\frac{\partial Z}{\partial y})^2 \end{cases} \quad (9)$$

are called metric coefficient and

$$\begin{cases} \beta_{xx} = \dfrac{\frac{\partial^2 Z}{\partial x^2}}{\sqrt{\alpha_{xx}\alpha_{yy} - \alpha_{xy^2}}}, \\ \beta_{xy} = \dfrac{\frac{\partial^2 Z}{\partial x \partial y}}{\sqrt{\alpha_{xx}\alpha_{yy} - \alpha_{xy^2}}}, \\ \beta_{yy} = \dfrac{\frac{\partial^2 Z}{\partial y^2}}{\sqrt{\alpha_{xx}\alpha_{yy} - \alpha_{xy^2}}}. \end{cases} \quad (10)$$

Eqns. (8) reduces to the standard formula for calculating the curvature at points along a curved line lying in the (x,y)-plane (Bergbauer, 2002; Roberts, 2001),

$$K = \frac{d^2y/dx^2}{(1+(dy/dx)^2)^{3/2}}. \tag{11}$$

Clearly, the curvature is directly related to the second derivative and thus highly sensitive to the noise. To overcome the noise, de-noising filters must be applied to the data. Fig. 1 shows the cross-section of the mapped surface. Gray vectors in this figure are perpendicular to the curve. Where these vectors are parallel (the curve is a flat or dipping plane) curvature has a value of zero. Where the vectors diverge (the curve forms an anticline or a ridge) the curvature is positive, and where vectors converge (the curve forms syncline or trough) the curvature is negative. For the surfaces at a particular point, depending on the orientation of the cross-section, an infinite number of curvatures can be calculated. The most useful curvatures are those described by planes perpendicular to the surface which are called normal curvatures (Roberts, 2001). There are different combinations of these normal curvatures which define some important characteristics of the surface. Here are some of the normal curvatures that help us to identify linear features of mapped surface.

Mean curvature, K_m

At any point on a surface, the average of both orthogonal normal curvatures is constant and it is called mean curvature (Bergbauer, 2002; Roberts, 2001):

$$K_m = \frac{K_1 + K_2}{2} = \frac{K_{max} + K_{min}}{2} = \frac{\alpha_{xx}\beta_{yy} + \beta_{xx}\alpha_{yy} - 2\alpha_{xy}\beta_{xy}}{2(\alpha_{xx}\alpha_{yy} - \alpha_{xy^2})}. \tag{12}$$

and in terms of the coefficients of a quadratic surface (Eq. 1) (Roberts, 2001),

$$K_m = \frac{a(1+e^2) + b(1+d^2) - cde}{(1+d^2+e^2)^{3/2}}, \tag{13}$$

K_1 and K_2 represent any pair of the orthogonal normal curvatures. K_{max} (the largest absolute curvature) is called the maximum curvature and K_{min} (perpendicular to the K_{max}) is called the minimum curvature. These two surface attributes are known as principal curvatures. In the following, we explain how the K_m can be used to derive maximum and minimum curvature.

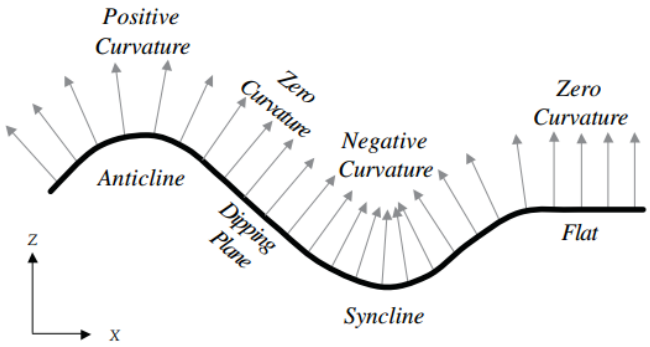

Figure 1. Schematic cross-section of the mapped surface (Roberts, 2001).

Gaussian curvature, K_g

This attribute is defined as the product of the principal curvatures. The name is due to the famous Gauss theorem that says: by bending the surface, the Gaussian curvature of the surface will remain constant until no breaking, stretching or compression occurs, (Bergbauer, 2002; Roberts, 2001). Then:

$$K_g = K_{max}K_{min} = \frac{\beta_{xx}\beta_{yy} - \beta_{xy}^{\ 2}}{\alpha_{xx}\alpha_{yy} - \alpha_{xy^2}}, \qquad (14)$$

and in terms of coefficients of quadratic surface (Eq. 1) (Roberts, 2001):

$$K_g = \frac{4ab - c^2}{(1 + d^2 + e^2)^2}. \qquad (15)$$

This attribute is used to determine the fault. However, in most cases due to the fluctuation of minimum curvature around zero value, K_g is not a useful attribute for fault detection but it is very important to calculate other curvature attributes.

Minimum and maximum curvatures are defined by the following formulas (Roberts, 2001):

$$K_{max} = K_m + \sqrt{K_m^{\ 2} - K_g}, \qquad (16)$$

$$K_{min} = K_m - \sqrt{K_m^{\ 2} - K_g}. \qquad (17)$$

These attributes are useful in determining linear features or lineaments such as fault, contact, etc.

Most positive and most negative curvatures, K_+ and K_-

To display the feature's edges of the mapped surface, we are looking for the most positive and most negative values from all feasible normal curvatures, which are called the most positive and most negative curvatures. For a quadratic surface, this can be calculated with zero setting of the coefficients d (Eq. 5) and e (Eq. 6) in equations (13) and (14). The result will be:

$$K_+ = a + b + \sqrt{(a-b)^2 + c^2}, \qquad (18)$$

$$K_- = a + b - \sqrt{(a-b)^2 + c^2}. \qquad (19)$$

Another way to calculate these attributes is to use the curvature matrix (Hansen and deRidder, 2006; Oruç et al., 2013). For a quadratic surface:

$$\begin{pmatrix} \frac{\partial^2 Z}{\partial x^2} & \frac{\partial^2 Z}{\partial x \partial y} \\ \frac{\partial^2 Z}{\partial x \partial y} & \frac{\partial^2 Z}{\partial y^2} \end{pmatrix} = \begin{pmatrix} 2a & c \\ c & 2b \end{pmatrix}. \qquad (20)$$

Eigenvalues of this matrix are equal to K_+ and K_- (Eq. (15) and (16)).

And for the general case (Oruç et al., 2013),

$$K_+ = \frac{1}{2}\left(\frac{\partial^2 Z}{\partial x^2} + \frac{\partial^2 Z}{\partial y^2} + \sqrt{\left(\frac{\partial^2 Z}{\partial x^2} - \frac{\partial^2 Z}{\partial y^2}\right)^2 + 4\left(\frac{\partial^2 Z}{\partial x \partial y}\right)^2}\right),$$

$$K_- = \frac{1}{2}\left(\frac{\partial^2 Z}{\partial x^2} + \frac{\partial^2 Z}{\partial y^2} - \sqrt{\left(\frac{\partial^2 Z}{\partial x^2} - \frac{\partial^2 Z}{\partial y^2}\right)^2 + 4\left(\frac{\partial^2 Z}{\partial x \partial y}\right)^2}\right). \qquad (21)$$

The diagonal form of this matrix is $\begin{pmatrix} K_+ & 0 \\ 0 & K_- \end{pmatrix}$ and its determinant is equal to $K_+ \times K_-$.

Shape index, SI

This attribute quantifies the local surface shape and describes the local morphology of the surface.

Barraud (2013) presented the range of the shape index values in terms of cap (0.875-1), dome (0.625-0.875), ridge (0.375-0.625), saddle ((-0.375)-0.375), rut ((-0.375)-(-0.625)), trough ((-0.625)-(-0.875)) and cup ((-0.875)-(-1)). The most negative and most positive curvatures can be combined with the following equation to get the shape index (Barraud, 2013):

$$\text{Shape index} = \frac{2}{\pi}\tan^{-1}\left(\frac{K_+ + K_-}{K_- - K_+}\right). \qquad (22)$$

3 Applying the method to the synthetic model

At this stage, the attributes discussed above were tested on a gravity anomaly produced by four cubes each having a density contrast of $0.5\,\mathrm{gr/cm^3}$ (Table 1).

Table 1. Properties of the synthetic model.

Model No.	Dimensions (km)	Depth (km)
1	$5\times22\times9.5$	0.5
2	$7\times7\times8.5$	1.5
3	$15\times7\times8$	2
4	$10\times5\times9$	1

The theoretical gravity anomalies are calculated using the algorithm given by Plouff (1976). Fig. 2 shows the anomaly map produced by cubes without the noise while the grid interval is 400 m. Attributes are calculated using the method described above and shown in Fig. 3. According to Fig. 3a, maximum values of the dip angle coincide with the edges of the anomalies. The result is similar to the horizontal gradient magnitude (HGM) except for the limited values of the inverse tangent function of the dip angle. Zero contours of the Gaussian curvature (solid black lines) are distorted near the edges of the anomalies and some additional zero contours are produced (Fig. 3b). This is because the minimum curvature values are small and fluctuate around zero. As a result, the Gaussian curvature's sign changes frequently which causes several additional contours outside the edges. Therefore, this attribute is not suitable for determining the boundaries of the anomaly. Zero contours of maximum curvature (solid black lines in Fig. 3c) and the most positive curvature (solid black lines in Fig. 3d) properly show the edges of the cubes. Figs. 3c and 3d show that over anomalies, a quadratic surface has negative curvature values and forms a ridge. It is flat or dipping plane over the edges of the anomalies with a zero curvature value and then, concavity changes to positive values. Zero contours of the curvature matrix determinant (solid black lines in Fig. 3e) show the edges of the anomalies but some additional zero contours appear. The shape index attribute quantifies the local shape of anomalies (Fig. 3f). As it is obvious from Fig. 3f, in cube 1, anomaly is ridge-like and near the end of the cube, it becomes dome-like. For cubes 3 and 4, the situation is the same but for cube 2, it is more dome-like rather than being ridge-like. Also, the range of anomaly is determined well except in the corners, as it does not satisfy the linearity assumption. Zero contours of the most positive curvature, zero contours of the tilt angle and maximum values of HGM are compared in Fig. 4. Maximum values of HGM (+ symbol) agreed with zero contours of the most positive curvature (solid red line), but zero contours of the tilt angle (solid blue line) are located outside the scope of the cubes. Zero contours of the maximum curvature are

approximately matched with the zero contours of the most positive curvature. As shown in the Figures 3 and 4, the results of the most positive and maximum curvatures have better compliance with the edges of the anomalies.

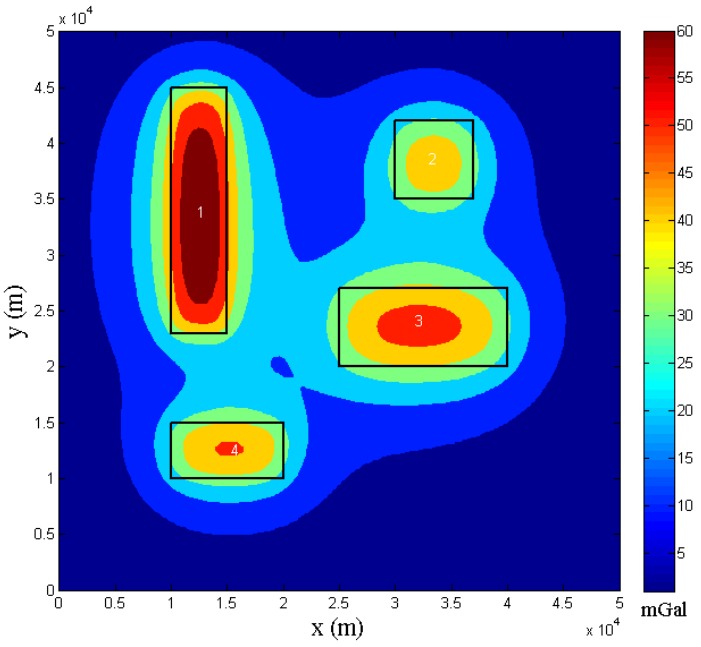

Figure 2. Gravity anomaly of the synthetic model. Black lines are outlines of the cubes.

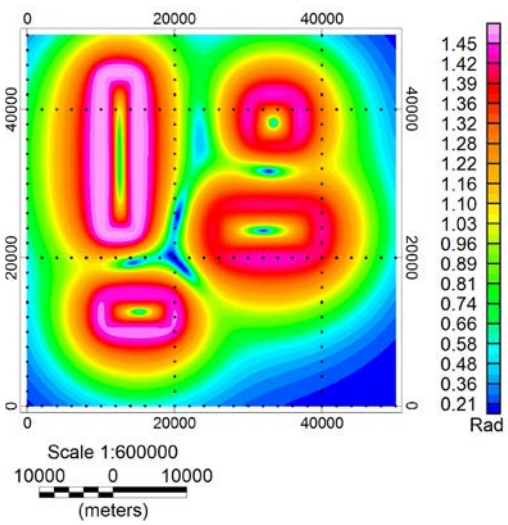

(a)

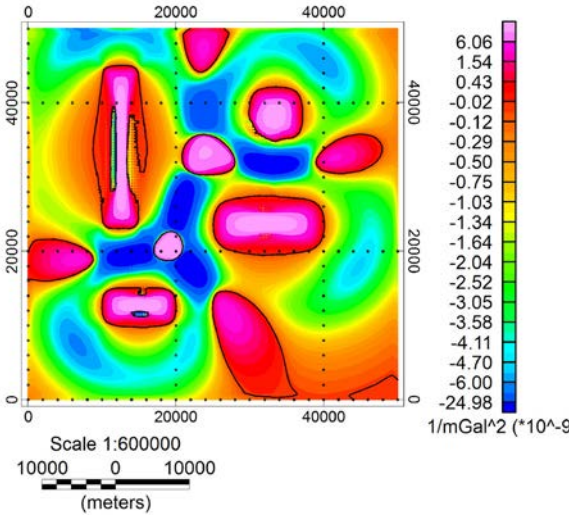

(b)

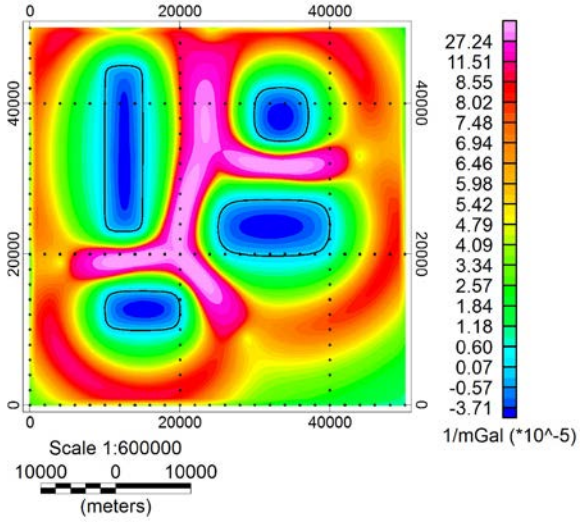

(c)

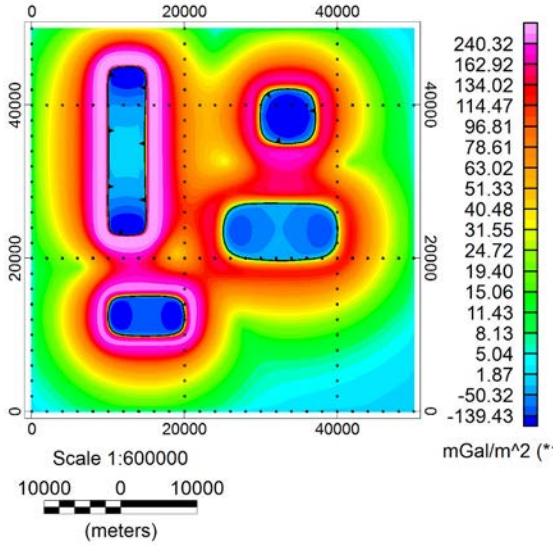

(d)

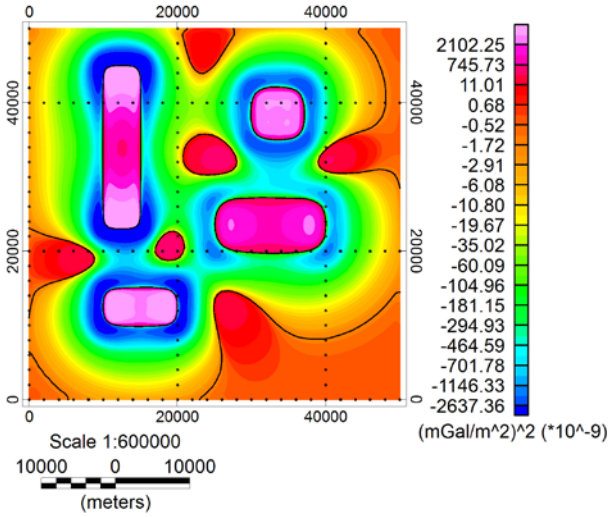

(e)

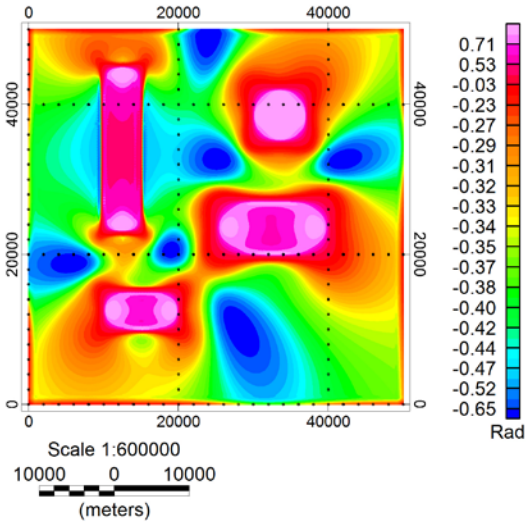

(f)

Figure 3. The surface-derived attributes maps over the synthetic model. (a) Dip angle. This attribute has its maximum value over the edges of cubes. (b) Gaussian curvature. (c) Maximum curvature. (d) Most positive curvature (e) Determinant of the curvature matrix. (f) Shape index. Values of the shape index determine the local shapes of the anomalies. Solid black lines in Gaussian curvature, maximum curvature, determinant and most positive curvature are zero contours which coincide with edge of the anomalies.

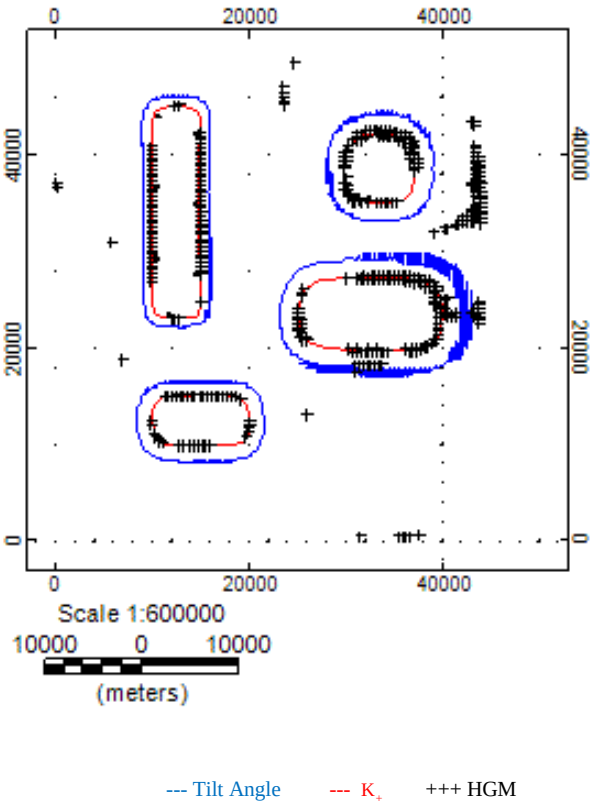

Figure 4. Comparison of the zero contours of most positive curvature (solid red line) and tilt angle (solid blue line) with maximum values of HGM (+ symbol).

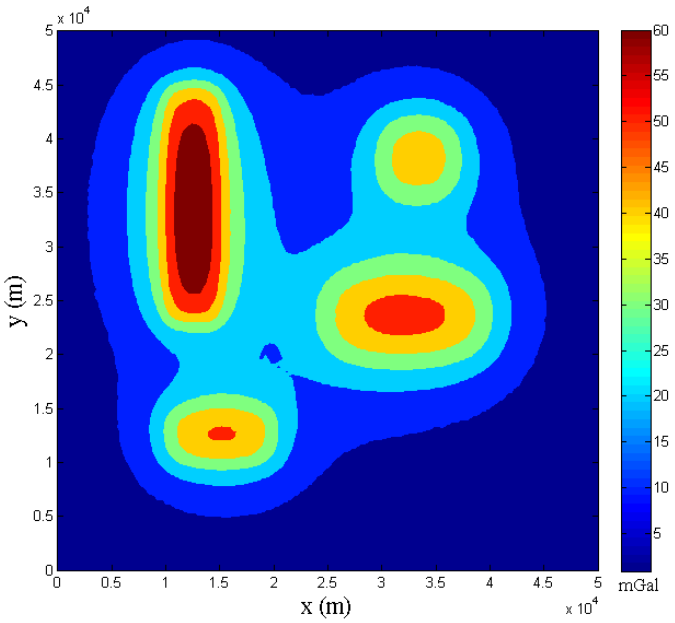

Figure 5. Gravity anomaly of cubes contaminated with Gaussian noise, with a mean of zero and standard deviation of 0.1mGal .

To evaluate the stability of the method in the presence of noise, a relatively high level of noise by Gaussian distribution with a mean of zero and standard deviation of 0.1 mGal was added to the synthetic data (Fig. 5.) Curvature attributes are calculated and shown in Fig. 6.

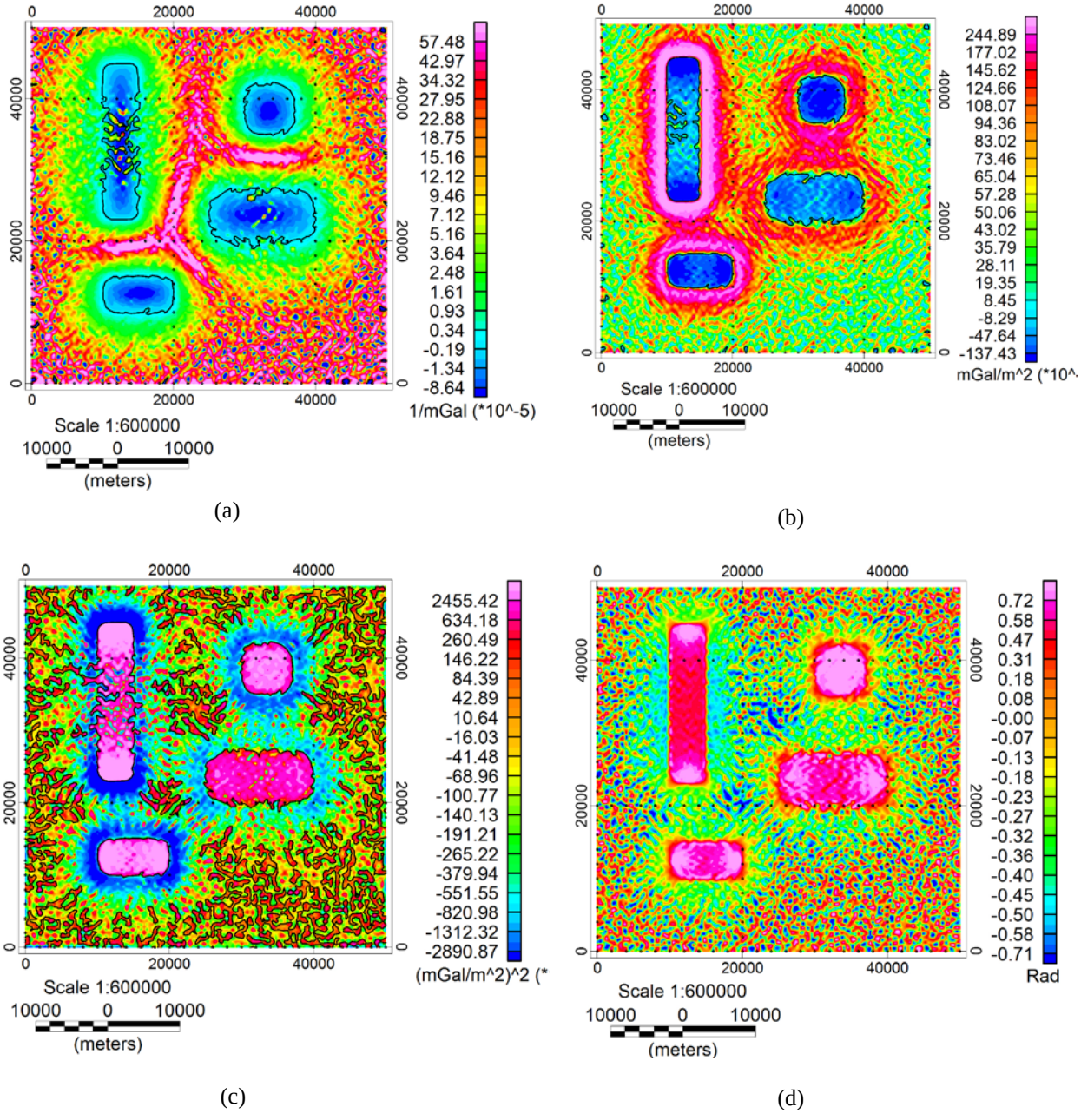

Figure 6. The surface-derived attributes calculated from noisy synthetic gravity data (Fig. 5). (a) Maximum curvature. (b) Most positive curvature. (c) Determinant of curvature matrix. (d) Shape index. Solid black lines in maximum curvature, determinant and most positive curvature are zero contours that coincide with the edges of anomalies.

As illustrated in Figure 6, the curvature attributes are slightly disturbed by the noise comparing with the results from applying to noise-free synthetic data. The reason is that the curvature attributes are obtained from the second derivatives and therefore sensitive to the noise. However, the results are still acceptable and trustworthy. The zero contours, as well, indicate locations of the edges. As shown in Fig. 6b, sensitivity of the zero contours of most positive curvature to noise is lower than that of the other zero contours. In case of highly noisy data sets, applying a low pass filter or upward continuation before applying the method is recommended.

4 Applying the method to real data

The method was applied to the residual anomaly map over a sulfide deposit in Noranda, Quebec, Mobrun ore (Grant and West, 1965). Data were collected on 13 profiles; the distance between the profiles and data on profiles was about 10 meters (Fig. 7). The average bulk density of mineral samples obtained from the boreholes was $4.6\,g/cm^3$ and the mean density of the host rock was $2.7\,g/cm^3$. The depth to top and base of the Mobrun sulfide body obtained by drilling information were 17m and 187m, respectively (Roy et al., 2000). Using the method described above, curvature attributes were calculated on this residual anomaly map. The results are shown in Fig. 8. Zero contours of the maximum and most positive curvature (solid black line) in Figs. 8a and 8b agree well, but zero contours of the curvature matrix determinant in Fig. 8c has some extra zero contours. The shape of the anomaly over the central part of the anomaly is a ridge (Fig. 8d). Comparison of Figs. 8a and 8e shows that the curvature can determine more lineaments from the surface without the dip saturation problem. A curvature does not have this problem, as it is completely independent from the direction of the surface (Roberts, 2001). Zero contours of the attributes are shown by solid black lines.

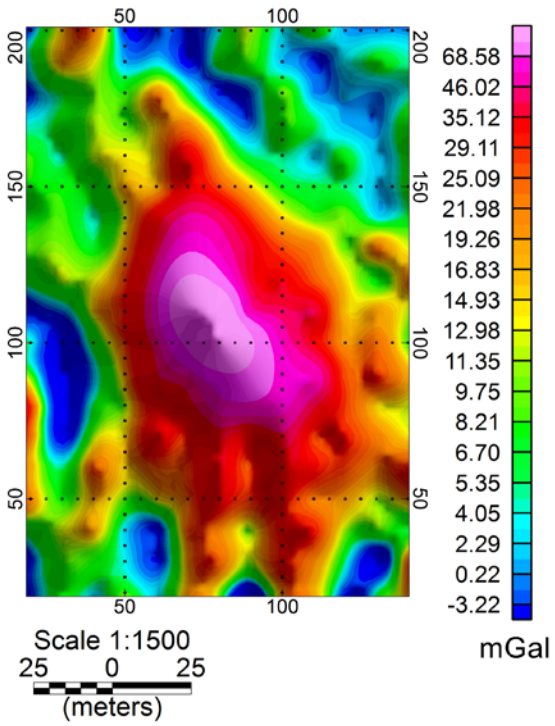

Figure 7. The residual anomaly map over a sulfide deposit, Noranda, Quebec, Mobrun ore.

In order to compare the results of the attributes, tilt angle and HGM maps are shown in Fig. 9. Comparing Fig. 8e and Fig. 9b, one can easily see the dip saturation problem in the dip angle. Fig. 9b shows that zero contours of the most positive curvature are well matched with the maximum values of HGM. Zero contours of the tilt angle and the most positive curvature are compared with maximum values of HGM (Fig. 10). As it can be seen, the results of these methods are almost identical.

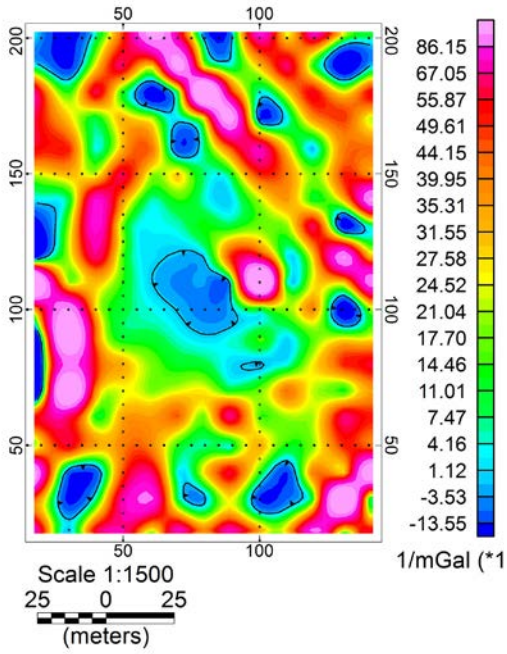
50
100
200
150
100
50
86.15
67.05
55.87
49.61
44.15
39.95
35.31
31.55
27.58
24.52
21.04
17.70
14.46
11.01
7.47
4.16
1.12
-3.53
-13.55
1/mGal (*1
Scale 1:1500
25 0 25
(meters)

(a)

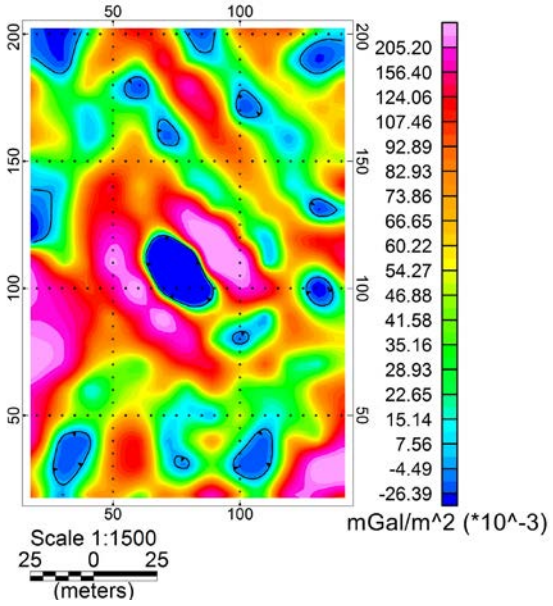
50
100
200
150
100
50
205.20
156.40
124.06
107.46
92.89
82.93
73.86
66.65
60.22
54.27
46.88
41.58
35.16
28.93
22.65
15.14
7.56
-4.49
-26.39
mGal/m^2 (*10^-3)
Scale 1:1500
25 0 25
(meters)

(b)

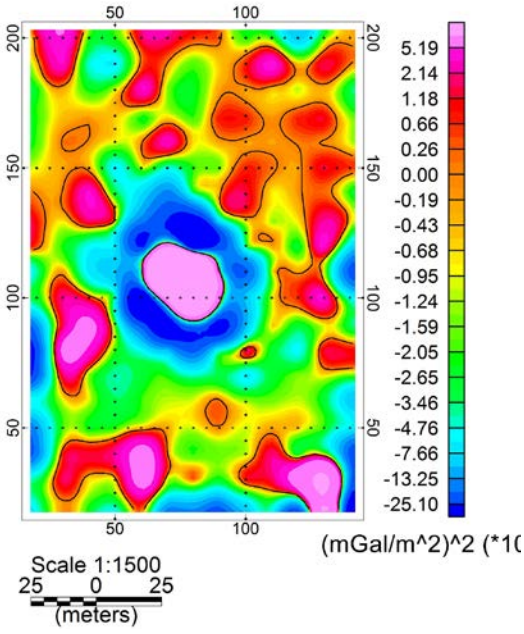
50
100
200
150
100
50
5.19
2.14
1.18
0.66
0.26
0.00
-0.19
-0.43
-0.68
-0.95
-1.24
-1.59
-2.05
-2.65
-3.46
-4.76
-7.66
-13.25
-25.10
(mGal/m^2)^2 (*1(
Scale 1:1500
25 0 25
(meters)

(c)

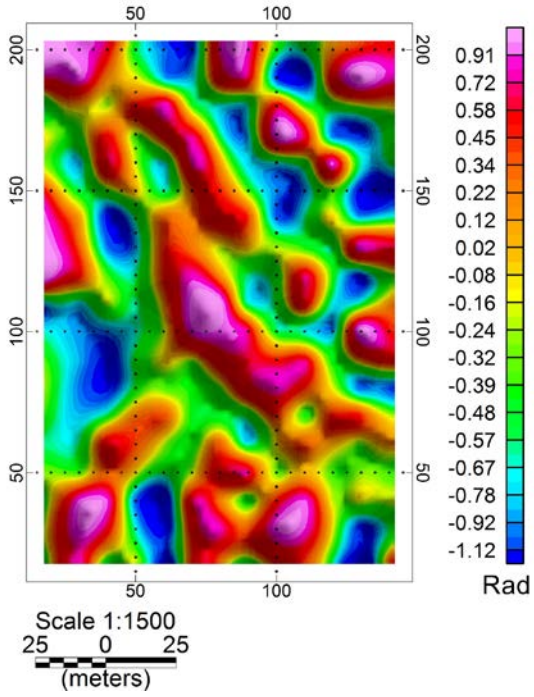
50
100
200
150
100
50
0.91
0.72
0.58
0.45
0.34
0.22
0.12
0.02
-0.08
-0.16
-0.24
-0.32
-0.39
-0.48
-0.57
-0.67
-0.78
-0.92
-1.12
Rad
Scale 1:1500
25 0 25
(meters)

(d)

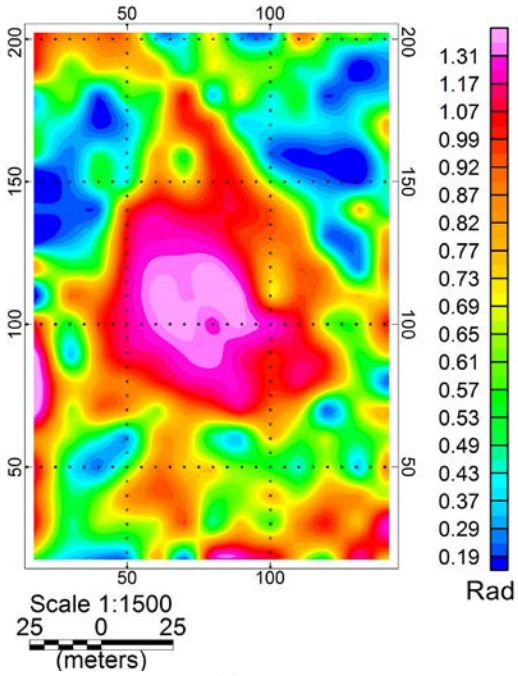

(e)

Figure 8. Curvature attributes calculated from the gravity residual anomaly map. (a) Maximum curvature. (b) Most positive curvature. (c) Determinant of curvature matrix. (d) Shape index. (e) Dip angle. Solid black lines are zero contours of the attributes.

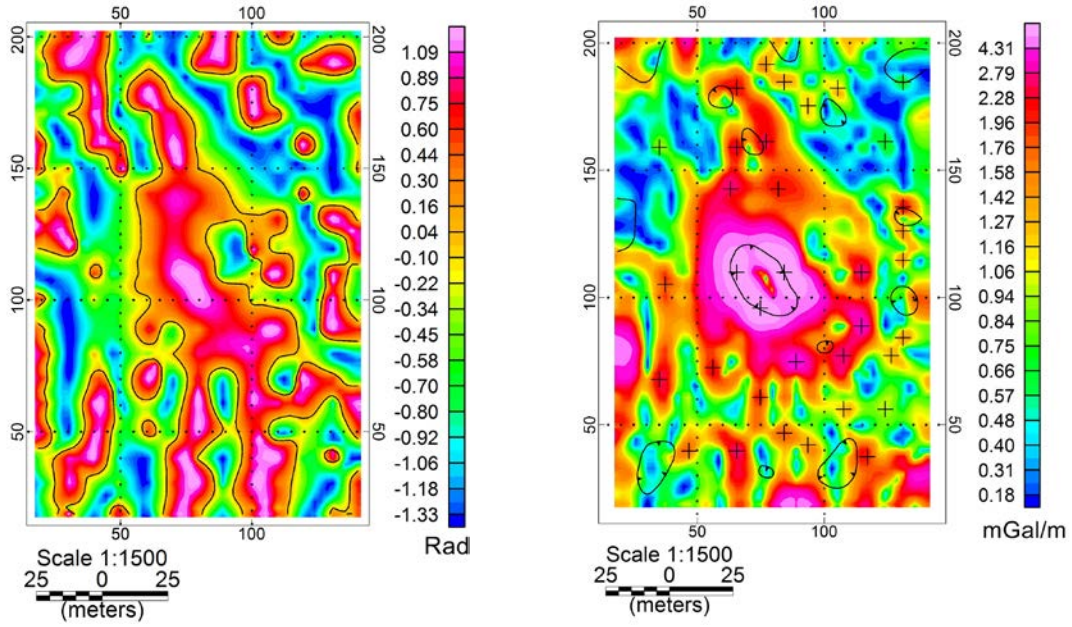

(a) (b)

Figure 9. (a) Tilt angle map. Solid black lines are zero contours. (b) HGM map. Solid black lines are zero contours of the most positive curvature. The (+) Symbols show maximum values of HGM.

5 Conclusions

In this paper, we introduced the surface-derived attributes that are useful to determine the linear features. The magnitudes of the normal curvature of the surface are calculated by two fundamental forms of the surface. In a special case, a quadratic surface is fitted to data and the coefficients of this surface are obtained with the least square method. These attributes are calculated by using these coefficients to show the areas with high curvature values that represent the linear features. The dip angle attribute which is being used widely in the interpretation of seismic data is similar to the horizontal gradient magnitude (HGM). However, as the inverse tangent function in the dip angle has limited values, this attribute has a saturation problem. Except for the zero contours of the Gaussian curvature map which has distortions around the edges of anomalies, zero contours of the most positive curvature, the determinant of curvature matrix and maximum curvature properly show the edges of anomalies. The shape index attribute also determines the local shape of the surface. The method was applied to the synthetic data with and without noise.

Finally, the curvature attributes were tested on real data from Mobrun massive sulfide ore of Canada. The results of the curvature attributes were compared with those of other conventional methods, such as the horizontal gradient magnitude (HGM) and tilt angle maps. All of these methods were matched with good accuracy in determining the boundaries of the anomalous sources.

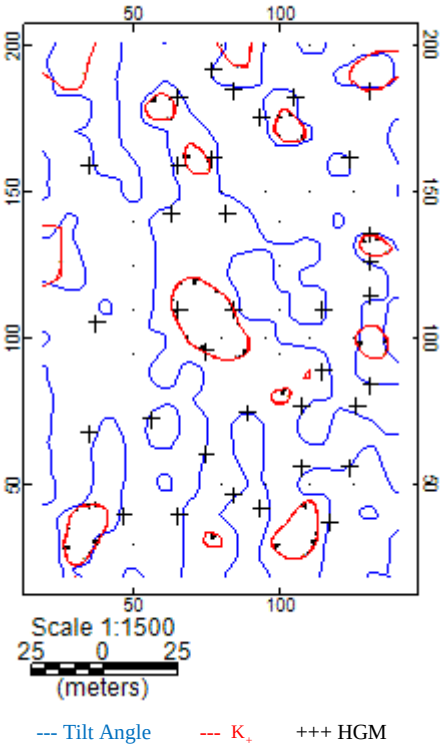

Figure10. Comparison of the zero contours of most positive curvature (solid red line) and tilt Angle (solid blue line) with maximum values of HGM (+ symbol).

References

Barraud, J., 2013, Improving identification of valid depth estimates from gravity gradient data using Curvature and Geometry analysis: First break, 31, 87–92.

Bergbauer, S., 2002, The use of curvature for the analyses of folding and fracturing with application to the emigrant gap anticline, Wyoming: Phd. thesis, Stanford University.

Cevallos, C., Kovac, p., Lowe, S. J., 2013, Application of curvatures to airborne gravity gradient data in oil exploration: Geophysics, 78, G81-G88.

Cooper, G. R. J., and D. R. Cowan, 2003, The application of fractional calculus to potential field data: Exploration Geophysics, 34, 51 –56.

Grant, F. S., and West, G. F., 1965, Interpretation theory in Applied Geophysics: McGraw-Hill. , 70, 39-43.

Grauch, V. J. S., and L. Cordell, 1987, Limitations of determining density or magnetic boundaries from the horizontal gradient of gravity or pseudo gravity data: Geophysics, 52, 118 –121.

Hansen, R. O., and E. deRidder, 2006, Linear feature analysis for aeromagnetic data: Geophysics, 71, no. 6, L61 –L67.

Marfurt, K. J., 2007, Seismic Attributes for Prospect Indentification and Reservoir Characterization: Society of Exploration Geophysics.

Miller, H. G., and Singh, V., 1994, Potential field tilt — A new concept for location of potential field sources: J. Applied Geophysics, 32, 213 –217.

Nabighian, M. N., 1972, The analytic signal of two-dimensional bodies with polygonal cross-section — Its properties and use for automated anomaly interpretation: Geophysics, **37**, 507–517.

Oruç, B., Sertçelik, I., Kafadar, Ö., and Selim, H. H., 2013, Structural interpretation of the Erzurum Basin, eastern Turkey, using curvature gravity gradient tensor and gravity inversion of basement relief: J. Applied Geophysics, 88, 105 –113.

Plouff, D., 1976, Gravity and magnetic fields of polygonal prisms and applications to magnetic terrain corrections: Geophysics, **41**, 727–741.

Phillips, J. D., Hansen, R. O., and Blakely, R. J., 2007, The use of curvature in potential-field interpretation: Exploration Geophysics, 38, 111 –119.

Roberts, A., 2001, Curvature attributes and their application to 3D interpreted horizons: First Break, **19**, 85–100.

Roy, L., Agarwal, B. N. P., and Shaw, R. K., 2000, A new concept in Euler deconvolution of isolated gravity anomalies: Geophysical Prospecting, **48**(3), 559-575.

Santos, D. F., Silva, J. B. C., Barbosa, V. C. F., and Braga, L. F. S., 2012, Deeppass — An aeromagnetic data filter to enhance deep features in marginal basins: Geophysics, 77, no. 3, J15 –J22.

Verduzco, B., Fairhead, J. D., Green, C. M., and MacKenzie, C., 2004, New insights to magnetic derivatives for structural mapping: The Leading Edge, **23**, 116 –119.

Wijns, C., C. Perez, and P. Kowalczyk, 2005, Theta map: Edge detection in magnetic data: Geophysics, **70**(4), L39 –L43.